Phase transitions under high pressure in binary Sn alloys (with In, Hg and Ga)

2002 J. Phys.: Condens. Matter 14 389

(http://iopscience.iop.org/0953-8984/14/3/309)

INSTITUTE OF PHYSICS PUBLISHING JOURNAL OF PHYSICS: CONDENSED MATTER

J. Phys.: Condens. Matter **14** (2002) 389–406 PII: S0953-8984(02)26754-5

Phase transitions under high pressure in binary Sn alloys (with In, Hg and Ga)

O Degtyareva[1], V F Degtyareva[1], F Porsch[2] and W B Holzapfel[3]

[1] Institute of Solid State Physics, Russian Academy of Sciences, Chernogolovka, Moscow District, 142432, Russia
[2] Mineralogisch-Petrologisches Institut, Universität-Bonn, 53113 Bonn, Germany
[3] FB 6 Physik, Universität-Paderborn, 33095 Paderborn, Germany

Received 9 July 2001, in final form 20 November 2001
Published 21 December 2001
Online at stacks.iop.org/JPhysCM/14/389

Abstract

Crystal structures of binary alloys of Sn with In, Hg and Ga were studied under pressure with diamond-anvil cells and energy-dispersive diffraction of synchrotron radiation. The ambient-pressure simple hexagonal (sh) phase in In–Sn alloys becomes unstable under pressure above 13 GPa and decomposes into the mixture of two phases: the body-centred tetragonal (bct) phase and hexagonal close-packed (hcp) phase with compositions ∼15 and ∼25 at.% In, respectively. The hcp/bct phase boundary shifts towards Sn with increasing pressure. A similar behaviour was found for the sh phase in Hg–Sn alloys, where the hcp phase occurs at higher pressure. Another bct phase with an axial ratio similar to that in In occurs under pressure in the Hg–Sn alloy system at the composition ∼50/50.

A sh phase was also found in the Ga–Sn alloy system near 80 at.% Sn at pressures above 11 GPa after heating to 150 °C, showing a similarity to the ambient-pressure sh phases in In–Sn and Hg–Sn alloys.

Structural sequences of phases in binary alloys are discussed with respect to the valence electron concentration of the alloys, taking into account the results of the present and previous structural high-pressure studies on Sn-based and related alloys.

1. Introduction

High-pressure studies have been focused so far mainly on elements or on compounds already existing at ambient pressure. Investigations on binary and multicomponent systems are still confined to a few selected compositions. Systematic studies on binary alloys under high pressure were developed by the group of Ponyatovskii using a 'pressure-quenching' method [1]. A series of intermediate high-pressure phases were obtained in alloys of the group I–V elements and a sequence of structures were determined with respect to the average number of valence electrons.

For a two-component system compared to a one-component system one should consider, in addition to the two thermodynamic variables pressure, P, and temperature, T, a third variable, composition, x. For a binary system this leads to an additional degree of freedom in phase equilibria and allows for new types of transformation under pressure, unlike those in a one-component system. For example, one can expect a single-phase formation from a two-phase mixture or a transition from one phase of a certain composition into two phases of different compositions.

Of special interest are studies on binary alloys of sp metals with relatively simple electron configuration. These metals correspond to the nearly-free-electron approach where only outer sp electrons participate in the bonding and determine the valence in density-of-states calculations. Binary alloys of the neighbouring elements in the periodic table, as for example In–Sn alloys, can be described using average parameters, such as average atomic volume and average number of valence electrons, and thus can be considered as 'model elements' with variable valency.

In this paper the results of structural high-pressure studies are presented for several binary alloys of Sn with a second component from the adjacent III and II groups (In, Hg and Ga). On the basis of the present and previous experimental results, phase stability is discussed with respect to alloy electron concentration for the phases occurring in these systems at ambient and high pressures.

2. Experimental procedure

Alloys of Sn with In, Hg and Ga were prepared by melting of appropriate amounts of the pure elements (5N purity). The phase content and lattice parameters of the alloys were examined under ambient conditions by means of x-ray diffraction on the diffractometer (SIEMENS D-500) and were found to correspond to their known phase diagrams [2, 3].

High-pressure studies were performed with diamond-anvil cells [4] and energy-dispersive x-ray diffraction (EDXD) using synchrotron radiation at DESY, HASYLAB [5, 6]. The ruby luminescence technique was used for pressure measurements with the nonlinear ruby scale [7]. The alloy samples were loaded into the gasket hole with mineral oil as the pressure-transmitting medium or without any transmitting medium. The high-pressure data for different alloy compositions of In–Sn and Hg–Sn were collected typically in two or three runs up to pressures of 30–37 GPa in steps of about 3 GPa on compression and of about 5 GPa on decompression. Data in transition regions were collected in steps of about 1 GPa. Some experiments were performed with diamonds with smaller tips of 300 μm diameter to reach pressures of about 68 GPa, using gold as an internal pressure marker. The diffraction spectra were evaluated with the computer programs EDXPowd and XPOWDER [8].

3. Results

The ambient-pressure phase diagrams for these three alloy systems In–Sn, Hg–Sn and Ga–Sn are shown in figure 1 [2,3]. Structural data on phases in these systems are taken from [9,10]. In the In–Sn alloy system three compositions are studied in the present work ($In_{10}Sn_{90}$, $In_{30}Sn_{70}$ and $In_{40}Sn_{60}$) in addition to the two compositions studied previously ($In_{20}Sn_{80}$ [11] and $In_{80}Sn_{20}$ [12]). In the Hg–Sn alloy system the composition $Hg_{15}Sn_{85}$ is studied in the present work, and our previous results for $Hg_{10}Sn_{90}$ [13] are reinterpreted in view of the present results. In the Ga–Sn alloy system the composition $Ga_{20}Sn_{80}$ is studied and results are reported.

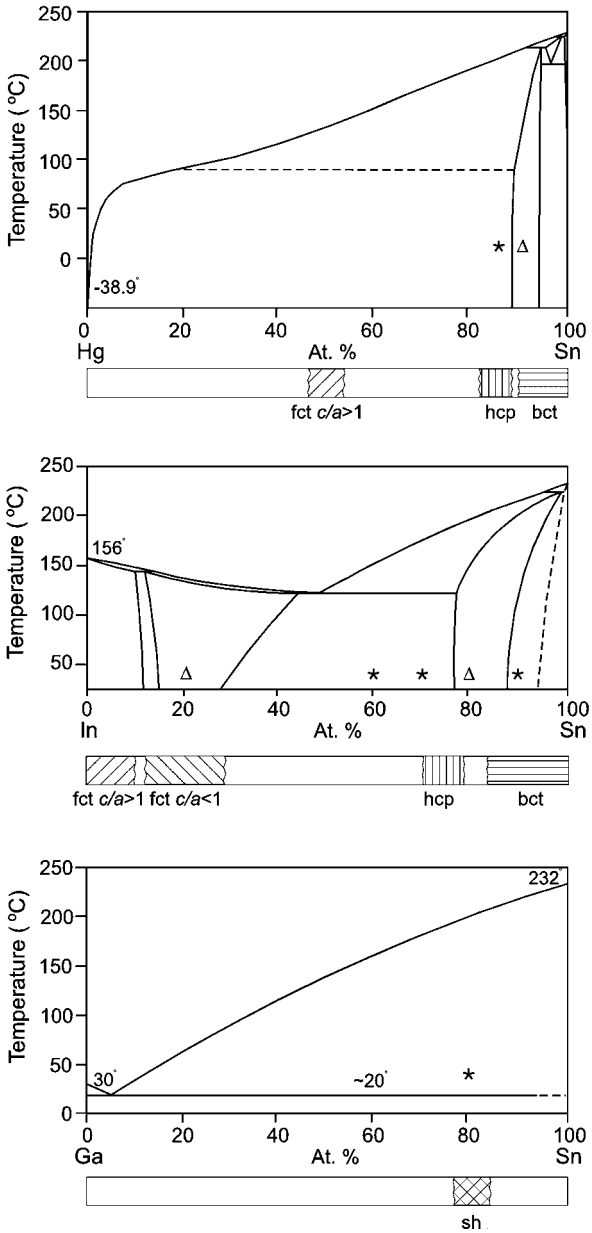

Figure 1. T–x phase diagrams for Hg–Sn, In–Sn and Ga–Sn alloy systems [2, 3]. The stars in the phase diagrams indicate the compositions of the alloys studied in the present work, while triangles indicate the compositions studied in previous works [11–13]. The plots below the diagrams show schematically regions of phase stability under pressure and the phase sequences with changing composition.

The following intermediate phases were observed in these alloy systems:

- simple hexagonal phase, sh, hP1, $P6/mmm$, $HgSn_9$ type;
- hexagonal close-packed phase, hcp, hP2, $P6_3/mmc$, Mg type;
- body-centred tetragonal phases, bct, tI2, $I4/mmm$, of two types:

In type related to fcc and designated as fct if $c/a > 1$ and fct′ if $c/a < 1$;
Sn II type related to bcc with $c/a < 1$ and designated as bct.

In the Sn-based alloys with In and Hg, a sh phase exists under ambient conditions in quite narrow regions of compositions corresponding to an electron concentration of 3.8 electrons/atom [2, 3]. Alloys containing only the single sh phase with compositions $In_{20}Sn_{80}$ and $Hg_{10}Sn_{90}$ were investigated previously [11, 13]. In the present work alloys of these systems are studied with compositions near to the sh phase region.

The Ga–Sn alloy system is of simple eutectic type at ambient pressure, but the formation of at least one new intermediate phase was expected under pressure, most probably the formation of a sh phase.

The sequences of phases with changing alloy composition found under high pressure in these alloy systems are shown schematically in the plots below the ambient-pressure phase diagrams in figure 1. Results obtained in these studies are summarized in table 1 and discussed below for each alloy system separately.

3.1. The In–Sn alloy system

At ambient pressure the In–Sn phase diagram contains intermediate phases in the following sequence: fct In solid solution with $c/a > 1$ up to 10 at.% Sn, fct′ with $c/a < 1$ in the range from 15 to 30 at.% Sn and a sh phase from ∼75 to ∼87 at.% Sn [9]. Sn forms solutes up to 3.3 at.% In in the *white-tin* structure. Our previous study [11] on a single-phase sh alloy of $In_{20}Sn_{80}$ composition has shown that sh decomposes above 13 GPa into a bct phase of Sn II type and a hcp phase. The latter was found to dominate with pressure increase and became a single phase above 23 GPa. This behaviour implies a shift of the hcp/bct two-phase region with pressure increase toward Sn. It is expected that single-phase regions for bct and hcp should exist at moderate pressure on both sides of the 80/20 composition. Therefore alloys of 10/90, 30/70, and 40/60 (In/Sn at.%) were prepared for the present studies.

$In_{10}Sn_{90}$. At ambient pressure the $In_{10}Sn_{90}$ alloy is composed of two phases: sh and β-Sn. The lattice parameters of the sh phase, $a = 322.04(6)$ pm, $c = 300.07(13)$ pm, $c/a = 0.932$, are close to the literature data for the Sn-rich boundary of the phase [9]. The lattice parameters of the β-Sn phase, $a = 582.60(12)$ pm, $c = 318.15(10)$ pm and $c/a = 0.546$, are close to the value for the In-rich boundary [9]. In accordance with these data, the phase compositions in the present $In_{10}Sn_{90}$ alloy correspond to ∼12 at.% In and ∼3 at.% In for sh and β-Sn, respectively.

The diffraction patterns of the $In_{10}Sn_{90}$ alloy at several pressures are shown in figure 2. A two-phase mixture, sh + β-Sn, is observed under pressure up to 9–11 GPa, where it transforms to a single phase with a bct structure of Sn II type. At pressures of about 48 GPa some extra peaks appear in addition to the peaks of the bct phase, and these new peaks grow with further increase in pressure at the expense of bct peaks. This new phase is indexed as hcp. Both phases, bct and hcp, are observed up to 68 GPa, the highest pressure reached in this study. Upon decompression the reverse transformation is observed: the hcp phase disappears at about 50 GPa, whereas the bct phase remains on further pressure decrease down to 10 GPa. At this pressure the original sh and β-Sn phases are recovered.

The high-pressure bct phase with the composition of 10 at.% In can be regarded as a solid solution of In in the bct form (Sn II)—a high-pressure form of tin above 10 GPa [14]. In our previous study on another In–Sn alloy with 20 at.% In, we have already observed a transformation from sh to bct with a small admixture of hcp [11]. We can conclude, therefore, that the solubility of In in this bct (Sn II) phase extends up to about 15 at.% In at pressures above 10 GPa.

Table 1. Characteristics of phases in the In–Sn and Hg–Sn alloys at ambient and high pressure. Structural data are shown at pressures for lower/middle/upper ranges of phase existence. Phase designation: sh—simple hexagonal, $P6/mmm$, hP1; hcp—hexagonal close-packed, $P6_3/mcm$, hP2; body-centred tetragonal, $P4/mmm$, tI2, where three types are distinguished and assigned: bct—related to bcc, with $c/a < 1$; fct—related to fcc, with $c/a > 1$; fct′—related to fcc, with $c/a < 1$ (lattice parameters for all three types are given in the bct setting); '+' indicates the presence of an additional phase; AP—ambient pressure.

Alloy system	Alloy composition studied (at.%)	Phase	Phase content (at.%)	Pressure range (GPa)	Lattice parameters under the given conditions				V_{at}, 10^6 (pm^3)	n (electrons /atom)	References
					a (pm)	c (pm)	c/a	P (GPa)			
In–Sn	$In_{80}Sn_{20}$	fct′	80/20	0–<30.1	345.61	441.41	0.903	AP	26.36	3.20	[12]
					313.44	389.0	0.878	30.1	19.11		
	$In_{40}Sn_{60}$	fct′+	∼72/28	0–<32.4	347.60	436.46	0.888	AP	26.37	3.28	
					328.1	404.3	0.871	13.8	21.7		
					313.0	382.8	0.865	32.4	18.75		
		sh+	∼22/78	0–12	321.31	299.55	0.933	AP	26.78	3.78	
					305.8	284.8	0.931	11	23.06		
		hcp+	∼25/75	13.8–<32.4	314.2	519.5	1.653	13.8	22.21	3.75	
			to ∼28/72		299.8	493.1	1.645	32.4	19.2	3.72	
	$In_{30}Sn_{70}$	fct′+	∼72/28	0–<36.5	347.59	436.86	0.889	AP	26.39	3.28	
					329.3	405.7	0.871	12.8	22.0		
		sh+	∼22/78	0–12.8	321.36	299.58	0.932	AP	26.79	3.78	
					304.5	284.4	0.932	12.8	22.8		
		hcp+	∼25/75	12.8–<36.5	315.8	521.1	1.650	12.8	22.5	3.75	
	$In_{20}Sn_{80}$	sh	20/80	0–13	321.7	299.8	0.932	AP	26.87	3.8	[11]
					307.7	287.1	0.933	12.8	23.53		
		bct+	∼15/85	10–23	367.61	331.12	0.901	13.3	22.37	3.85	[11]
					358.40	325.42	0.908	23.0	20.9		
		hcp+	∼25/75	10–23	315.16	519.67	1.649	13.3	22.35	3.75	[11]
		hcp	∼20/80	23–<30	302.00	495.94	1.642	31.0	19.58	3.80	
	$In_{10}Sn_{90}$	β-Sn+	∼5/95	0–9	582.60	318.15	0.546	AP	27.00	3.95	
					559.5	304.8	0.545	9.0	23.86		
		sh+	∼12/88	0–9	322.04	300.07	0.932	AP	26.95	3.88	
					309.0	288.6	0.934	9.0	23.87		
		bct	10/90	11–47	369.1	334.8	0.907	11.4	22.8	3.90	
		bct+	∼8/92	47–<68	339.7	314.8	0.927	48.3	18.16	3.92	
					328.6	304.6	0.927	68	16.45		
		hcp+	∼12/88	47–<68	296.6	476.6	1.610	48.3	18.15	3.88	
					285.5	465.2	1.63	68	16.42		
Hg–Sn	$Hg_{15}Sn_{85}$	sh+	∼11/89	0–17.4	320.05	298.14	0.932	AP	26.45	3.78	
					299.61	279.9	0.934	17.4	21.76		
		bct+	∼12/88	17.4–<36.3	361.6	327.3	0.905	17.4	21.4	3.77	
					349.4	319.7	0.915	33.3	19.51		
		fct+	∼50/50	17.4–<36.3	298.1	459.0	1.089	17.4	20.2	3.0	
					290.0	436.8	1.065	33.3	18.35		
	$Hg_{10}Sn_{90}$	sh	10/90	0–14	320.8	298.5	0.930	AP	26.6	3.80	[13]
					302.71	282.23	0.932	13.7	22.39		
		bct	10/90	14–55	365.5	331.4	0.907	13.7	22.14	3.80	[13]
		bct+	to ∼9/91	55–<66.4	∼ 330	∼ 305	∼ 0.92	66.4	16.6	3.82	
		hcp+	∼12/88	55–<66.4	285.3	466.8	1.636	66.4	16.45	3.76	

$In_{30}Sn_{70}$ and $In_{40}Sn_{60}$. At ambient pressure these alloys each consist of a two-phase mixture of sh and fct′ with $c/a < 1$. The sh phase has a phase composition close to the In-rich boundary

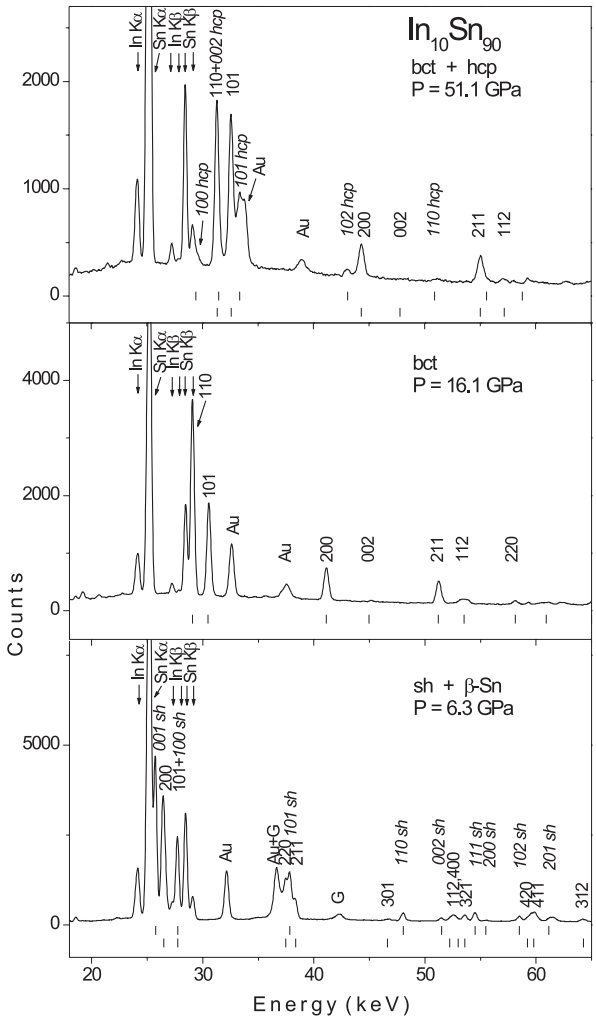

Figure 2. EDXD spectra of $In_{10}Sn_{90}$ collected on pressure increase with $2\theta = 9.50^{\circ}$ ($Ed = 7488.8$ keV pm). Fluorescence peaks from Sn and In are marked by arrows. The pattern at 6.3 GPa contains two phases: sh with $a = 311.8(2)$ pm, $c = 290.8(1)$ pm, $c/a = 0.933$; and β-Sn with $a = 565.3(7)$ pm, $c = 307(1)$ pm. At 16.1 GPa, a bct phase of Sn II type is observed with $a = 364.2(3)$ pm, $c = 333.1(5)$ pm, $c/a = 0.915$. The pattern at 51.1 GPa shows a two-phase mixture: bct of Sn II type with $a = 338.0(1)$ pm, $c = 313.4(1)$ pm, $c/a = 0.927$; and hcp with $a = 294.1(2)$ pm, $c = 475.9(4)$ pm, $c/a = 1.618$. The calculated peak positions are shown as tick marks below each pattern. Peak indices are indicated as *hkl* for bct and as *hkl* sh and *hkl* hcp for sh and hcp, respectively. 'G' denotes a diffraction peak from the gasket; 'Au' denotes diffraction peaks from the pressure marker gold.

of ∼75–77 at.% Sn, and the fct′ phase has a composition of ∼29 at.% Sn [9]. Under pressure, this two-phase mixture is observed up to pressures of about 11–13 GPa in both alloys. Above this pressure a change in the diffraction pattern is noticed, indicating the presence of a two-phase mixture involving the low-pressure fct′ phase and a new phase with hcp structure. This phase mixture, fct′ + hcp, is observed up to the highest pressure of 32 GPa reached in these runs for $In_{40}Sn_{60}$ and 37 GPa for $In_{30}Sn_{70}$. On pressure decrease, the reverse transitions are observed, recovering the initial two-phase mixture, fct′ + sh, on pressure release.

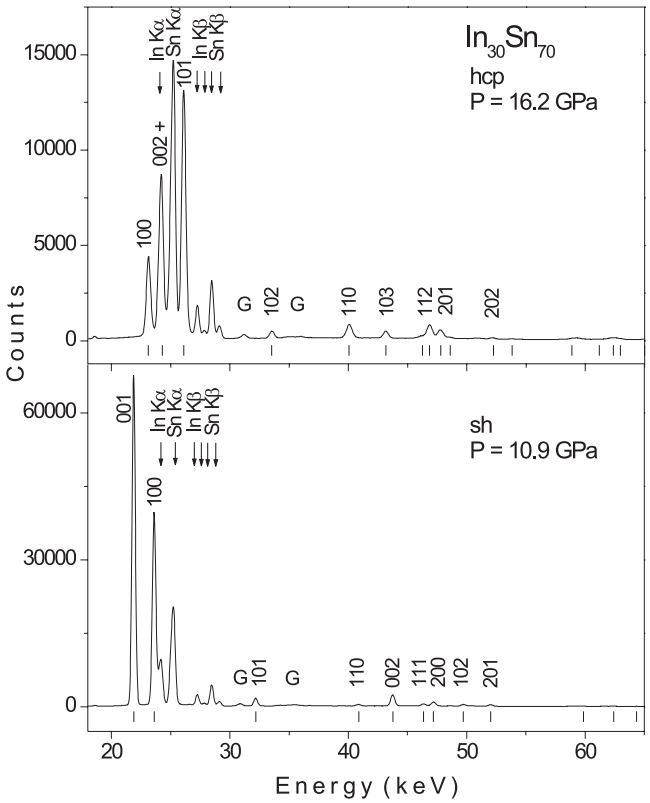

Figure 3. EDXD spectra of $In_{30}Sn_{70}$ collected on increasing pressure with $2\theta = 11.33^\circ$ ($Ed = 6280.2$ keV pm). Fluorescence peaks from Sn and In are marked by arrows. The pattern at 10.9 GPa is typical for the sh phase with $a = 307.3(1)$ pm, $c = 287.0(1)$ pm, $c/a = 0.934$. At 16.2 GPa the hcp phase has $a = 313.7(1)$ pm, $c = 517.0(3)$ pm, $c/a = 1.648$. The calculated peak positions are shown as tick marks below each pattern. 'G' denotes diffraction peaks from the gasket.

In another run on the $Sn_{70}In_{30}$ alloy, only the sh phase was observed under ambient conditions. This could result from slight differences in alloy composition (of the tiny piece loaded into the cell) due to the two-phase mixture in the initial alloy. The loaded sample apparently contained the sh phase corresponding to the In-rich boundary composition (around 75 at.% Sn). Therefore a transformation from sh to hcp was observed in this sample with no visible admixture of the fct′ phase. In figure 3 the diffraction patterns for this sample show a direct transition from sh to hcp.

The atomic volumes determined from diffraction patterns for fct′ and for sh transforming to hcp under pressure are shown in figure 4. The P–V data can be fitted within the present accuracy by any of the common second-order equations of state (EoS) [15,16]. These fitted EoS curves for fct′ and sh/hcp are nearly parallel to each other, indicating no change in compositions with pressure. The composition of the fct′ phase remains therefore close to 30 at.% Sn. The hcp phase corresponds to a composition of about 75 at.% Sn just after the appearance at 13 GPa and remains at near the same composition with pressure increase. The lattice parameters of the hcp phase observed in $In_{40}Sn_{60}$ are the same as for the $In_{30}Sn_{70}$ alloy and are also close to those observed for the Sn-rich alloy $In_{20}Sn_{80}$ [11] indicating that the hcp phase occurs in a very narrow range of compositions of about 5 at.%. Under pressure the composition range of the hcp phase widens slightly and shifts to the Sn-rich side.

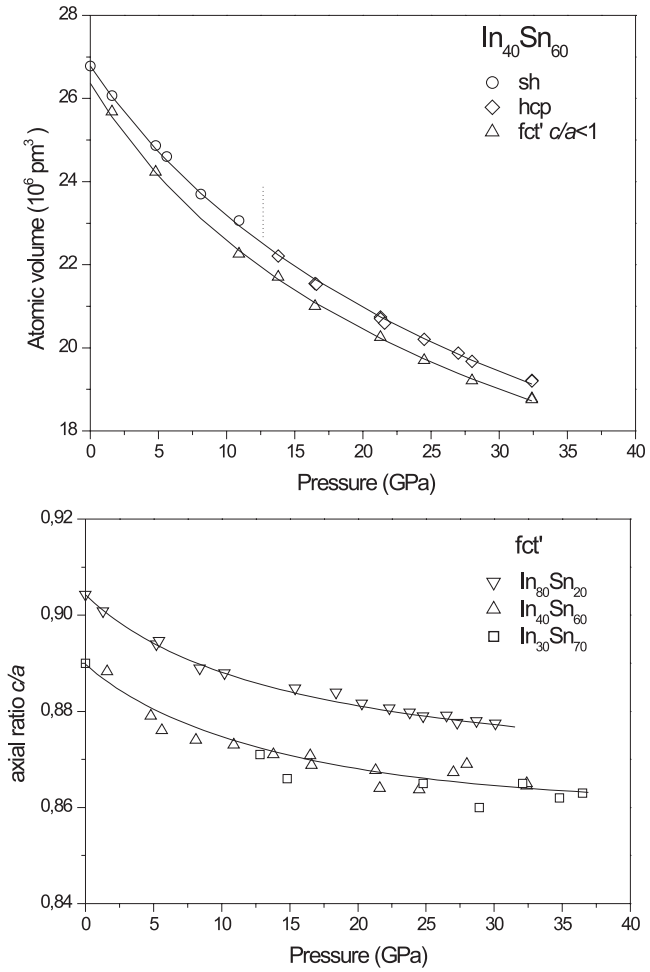

Figure 4. Upper panel: the effect of pressure on the atomic volume of $In_{40}Sn_{60}$ in the fct′, sh and hcp phases. The data were fitted with EoS, discussed in the text, which give the values for the atomic volume, bulk modulus and its pressure derivative: $V_0 = 26.78 \times 10^6$ pm^3, $K_0 = 48.1$ GPa, $K_0' = 3.6$ for sh/hcp; and $V_0 = 26.37 \times 10^6$ pm^3, $K_0 = 55.0$ GPa, $K_0' = 3.1$ for fct′. Lower panel: axial ratios for the fct′ phases in $In_{40}Sn_{60}$ and $In_{30}Sn_{70}$ alloys, observed in a mixed two-phase state. The composition of the fct′ phase is close to 30 at.% Sn. The data are compared with results for $In_{80}Sn_{20}$, where the fct′ phase was observed as a single phase [12].

The difference in atomic volume between the fct′ and hcp phases remains nearly constant over the whole range of pressures, as seen in figure 4. This value, $\Delta V \approx 0.46 \times 10^6$ pm^3, corresponds to a difference in composition for the fct and hcp phases of about 40–50 at.% following Vegard's law. This agrees with the assigned compositions of 30 at.% Sn for the fct′ phase and 75 at.% Sn for the hcp phase.

The variations of the c/a ratio for the fct′ phases (30 at.% Sn) in both alloys, $In_{40}Sn_{60}$ and $In_{30}Sn_{70}$, are shown in figure 4 in comparison with the previous data for the pure fct′ phase in an In alloy with 20 at.% Sn [12]. With pressure increasing, the axial ratio c/a decreases, i.e. the tetragonal distortion increases. The higher the Sn content in the fct′ phase, the lower the c/a ratio, which means an increase of the tetragonal distortion with Sn content.

3.2. The Hg–Sn alloy system

The Hg–Sn alloy system has an intermediate sh phase in a narrow concentration range from 5.5 to 11 at.% Hg (or 89–94.5 at.% Sn) [3] (figure 1). Our previous high-pressure studies on $Hg_{10}Sn_{90}$ alloy have shown a transition from this sh phase to a bct phase, regarded as a solid solution based on Sn II [13]. This, together with studies on $In_{20}Sn_{80}$, has shown that the degree of tetragonal distortion (c/a) is related to the average number of valence electrons, n, in the alloy. For $In_{20}Sn_{80}$ and $Hg_{10}Sn_{90}$ alloys the average number of valence electrons n is equal to 3.8. To provide further support of this model, another Hg–Sn alloy of higher Hg content (15 at.%) was studied in the present work.

Since the alloy system In–Sn has shown a new intermediate phase with hcp structure under pressure in the composition range of about 20–30% In, i.e. at $n \approx 3.75$, it was expected that high-pressure studies on Hg–Sn alloys with 10–15 at.% Hg may also reveal a new intermediate phase with hcp structure.

$Hg_{15}Sn_{85}$. The initial alloy $Hg_{15}Sn_{85}$ contains a sh phase with a very minor admixture of another phase (with an undetermined structure [3]). This sh phase persists with increasing pressure up to 14.5 GPa. At higher pressures a set of new diffraction peaks appears and coexists with the sh peaks up to ∼20 GPa. Above 20 GPa one set of diffraction peaks corresponds to a bct phase (Sn II) previously found in the $Hg_{10}Sn_{90}$ alloy under pressure. The remaining diffraction peaks were indexed to another bct phase with a crystal structure of In type, assigned as fct. At 20.4 GPa the lattice parameters are: for bct Sn, $a = 358.8(2)$ pm, $c = 326.4(6)$ pm, $c/a = 0.910$; and for bct In, $a = 296.6(6)$ pm, $c = 451.0(10)$ pm, $c/a = 1.521$ (in the fct setting, $c/a = 1.075$). On decompression the reverse transitions were observed and the sh phase was recovered (with a minor admixture of the unknown phase). Figure 5 shows the diffraction patterns of this alloy at ambient pressure with the sh phase and at 20.4 GPa containing two phases (bct + fct).

These two high-pressure phases were observed up to 36.3 GPa, the highest pressure of this study. The axial ratios for both bct phases vary only slightly with pressure. For bct Sn, c/a increases up to 0.915 and, for bct In, c/a decreases down to 1.507 (1.065 in the fct setting) (figure 6). The sh phase shows only a slight increase in the axial ratio from 0.931 at ambient pressure to 0.934 at 14.5 GPa (figure 6).

The results on the $Hg_{15}Sn_{85}$ alloy show that the ambient-pressure sh phase decomposed into two high-pressure phases. One of them is Sn rich with a composition of about 10/90 and can be regarded as a Sn II-based solid solution. The other phase is of In type (fct with $c/a > 1$) and probably has an alloy composition close to 50/50. This conclusion is consistent with the observation of the In-type structure in indium and In-rich alloys (with Cd, Sn or Pb) in the range of electron concentration 2.95–3.1 electrons/atom [9].

The data on atomic volume and axial ratio dependencies on pressure for the fct In-type phase in the Hg–Sn alloy, shown in figure 6, are very close to those observed for pure In [17–19], supporting the assumption of a ∼50/50 composition for this phase.

$Hg_{10}Sn_{90}$ (re-indexing of previous data and comparison with $In_{20}Sn_{80}$). Our previous work [13] reported results on $Hg_{10}Sn_{90}$ with the observation of a transformation from a sh phase to a bct phase of Sn II type at ∼15 GPa, and with evidence for a further transformation at a higher pressure around 55 GPa. The latter was tentatively interpreted as a transition to a single phase, probably with orthorhombic structure. This interpretation must be revised in view of our later [11] and present studies. Now we conclude that the diffraction patterns of the alloy $Hg_{10}Sn_{90}$ above 55 GPa should be interpreted as a two-phase mixture of a bct phase

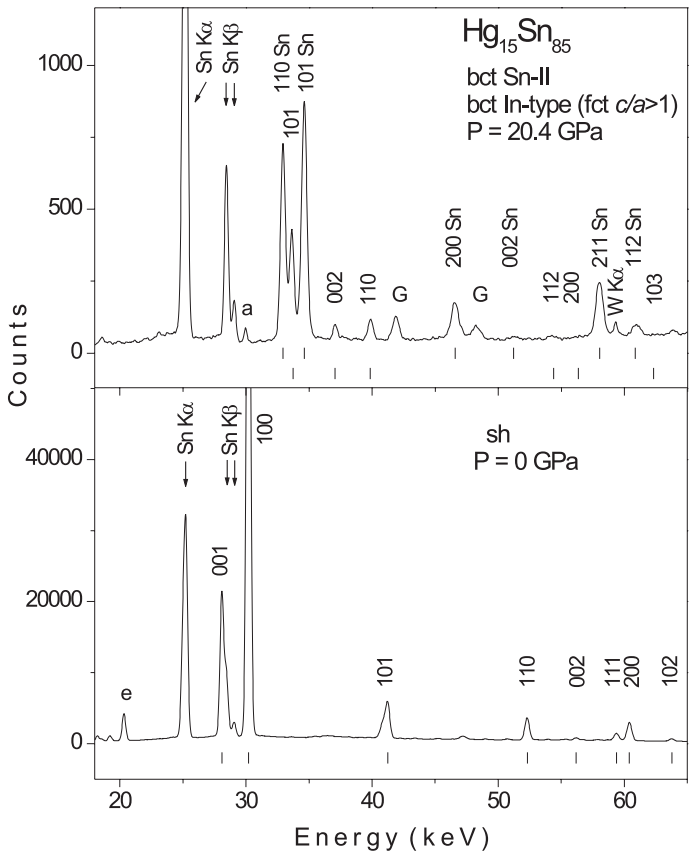

Figure 5. EDXD spectra of $Hg_{15}Sn_{85}$ collected on increasing pressure with $2\theta = 8.51^\circ$ ($Ed = 8354.1$ keV pm). Fluorescence peaks from Sn are marked by arrows. At ambient pressure the sh phase has $a = 319.5(2)$ pm, $c = 297.4(2)$ pm. At 20.4 GPa two bct phases exist: bct (Sn II type) with $a = 358.8(2)$ pm, $c = 326.4(6)$ pm, $c/a = 0.910$ (peaks hkl Sn); and bct (In type) with $a = 296.6(6)$ pm, $c = 451(1)$ pm, $c/a = 1.075$ in the fct setting (peaks hkl). 'e' denotes an escape peak, 'a' denotes an electronic artifact observed with this set-up at low count rates.

of Sn II type, observed at lower pressure, and a new intermediate phase with hcp structure. Figure 7 shows a diffraction pattern from the previous work [13], reinterpreted as a two-phase mixture of bct (Sn II-type) and hcp phases.

In the related In–Sn system the intermediate phase with hcp structure appears under pressure, and exists over a narrow range of composition around 75 at.% Sn, i.e. at the average number of valence electrons $n = 3.75$. In the Hg–Sn system the hcp phase was observed in the $Hg_{10}Sn_{90}$ alloy (at $n = 3.8$) in a mixture with another Sn-enriched phase. This indicates that the hcp phase corresponds to a composition of about 15/85 (Hg/Sn), and thus one can conclude that the hcp phase appears in the Hg–Sn alloy at $n = 3.75$. Therefore, a complete transformation to hcp is expected in the alloy $Hg_{15}Sn_{85}$ at pressure above 50–60 GPa.

These hcp phases with nearly ideal c/a ratios (1.636 for Hg–Sn and 1.641 for In–Sn) should be considered as high-pressure intermediate phases in these alloy systems, since the pure elements Sn and In are known not to transform to hcp structure, whereas the hcp phase of Hg appears at ∼36 GPa with $c/a = 1.74$ [20].

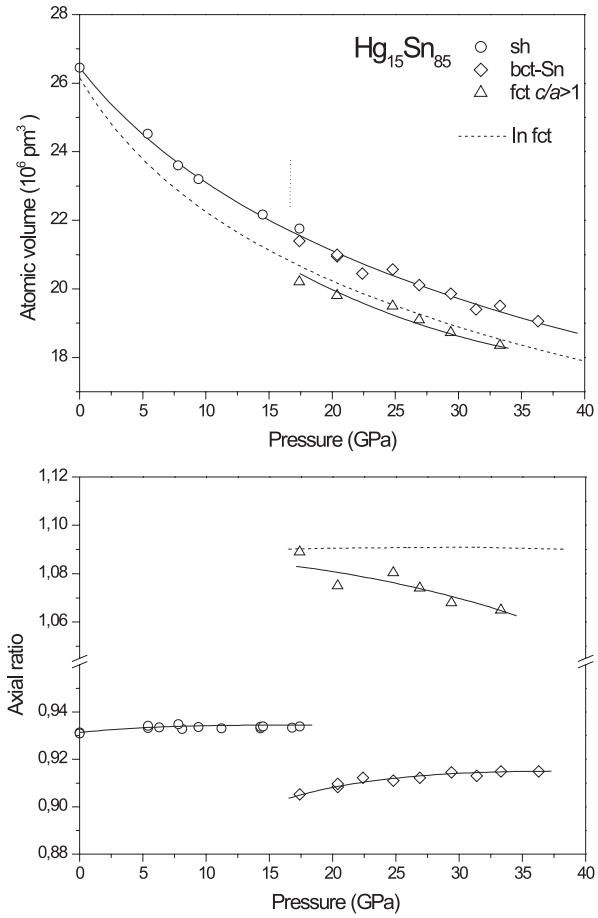

Figure 6. Upper panel: the effect of pressure on the atomic volume of $Hg_{15}Sn_{85}$ in the sh, bct and fct structures, together with the data for pure In [17, 18]. The data have been fitted with second-order EoS, discussed in the text, which give the values for the atomic volume, bulk modulus and its pressure derivative: $V_0 = 26.45 \times 10^6$ pm^3, $K_0 = 56(3)$ GPa, $K_0' = 4.1(3)$ for sh/hcp; and for the fct phase of In type: $V_0 = 26.16 \times 10^6$ pm^3, $K_0 = 41.8(5)$ GPa, $K_0' = 4.81(6)$, similar to the data for pure In [17, 18]. Lower panel: axial ratios for sh, bct (Sn II-type) and fct (In-type) phases (fct setting) in $Hg_{15}Sn_{85}$ together with literature data for c/a for In [17, 18] in the corresponding pressure range.

Phase diagrams for In–Sn and Hg–Sn under pressure

All these data together allow us to draw schematically the regions of phase existence using pressure–composition (P–x) coordinates. Without kinetic studies it is difficult to determine precisely the thermodynamic equilibrium lines, and therefore the present P–x diagrams primarily determine the topology of the corresponding phase regions and do not yet give precise values for these boundaries.

For the In–Sn system the corresponding figure 8 shows the formation of a new intermediate phase with the hcp structure at the composition of about 75 at.% Sn, extension of the In solubility in the bct phase (Sn II) and a shift of the hcp/bct phase boundary towards Sn with increasing pressure. The fct′ phase ($c/a < 1$) shows a stability region for compositions of <30 at.% Sn.

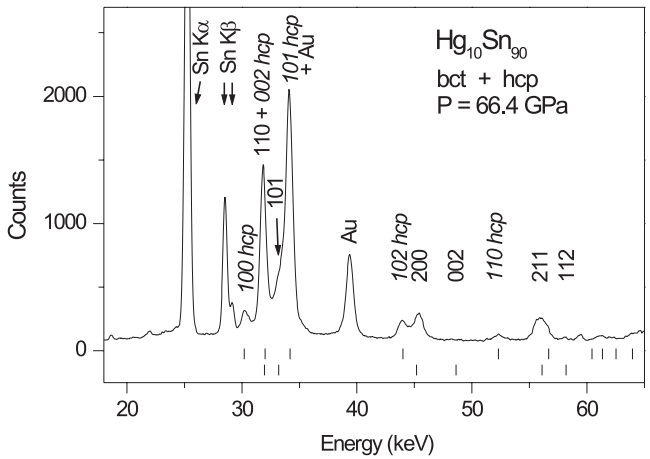

Figure 7. The EDXD spectrum of $Hg_{10}Sn_{90}$ from the previous work [13] collected at 66.4 GPa with $2\theta = 9.52^\circ$ ($Ed = 7465$ keV pm). Fluorescence peaks from Sn are marked by arrows. The two-phase mixture of the bct phase with a small amount of hcp phase is illustrated: bct with $a = 330(1)$ pm, $c = 307(4)$ pm (peaks hkl); and hcp with $a = 285.3(2)$ pm, $c = 466.8(6)$ pm (peaks hkl hcp). The calculated peak positions are shown as tick marks below the pattern. 'Au' denotes diffraction peaks from the pressure marker, gold.

The P–x phase diagram for the Hg–Sn system (figure 9) shows destabilization of the sh phase under pressure and the formation of two intermediate phases: one with the In-type structure (fct with $c/a > 1$) at a composition of about 50 at.% Sn; and the other with the hcp structure at a composition of about 85 at.% Sn. The diagram shows an extension of the Hg solubility in bct Sn II above 10 at.%.

These diagrams for In–Sn and Hg–Sn show close similarities in structural sequences with respect to alloy composition, especially if chemical composition is replaced by average valence electron concentration.

3.3. The Ga–Sn system

The Ga–Sn system has a phase diagram of simple eutectic type at zero pressure [3] (figure 1). However, in the In–Sn system an intermediate phase has occurred on the Sn-rich side (around 20 at.% In) already at zero pressure [3]. In accordance with the 'homology rule' for T–x–P diagrams, the effect of pressure is often similar to a replacement of one of the constituents by a heavier element from the same group in the periodic table [1]. Therefore, one can expect an intermediate sh phase to possibly occur in the Ga–Sn system under pressure; it would be similar to the In–Sn intermediate sh phase at zero pressure.

Therefore a $Ga_{20}Sn_{80}$ alloy has been studied up to 24 GPa without and with heating under pressure. Initially the alloy contains β-Sn and Ga; the latter was not identified in diffraction patterns, because of strong texture or possibly the occurrence of a liquid state. However, at pressures around 23 GPa a bct Ga phase (In type) was observed (figure 10) with lattice parameters in agreement with the data on pure Ga [21, 22]. The transformation of the β-Sn component to the bct Sn structure occurred at about 10–13 GPa as in pure Sn [14]. The values for the volume and c/a for the bct Sn phase in the $Ga_{20}Sn_{80}$ alloy coincide with the values for pure Sn, and one can conclude that this phase does not form solutes in Ga to any substantial degree. On decompression the reverse transformation is observed, and the initial state is recovered.

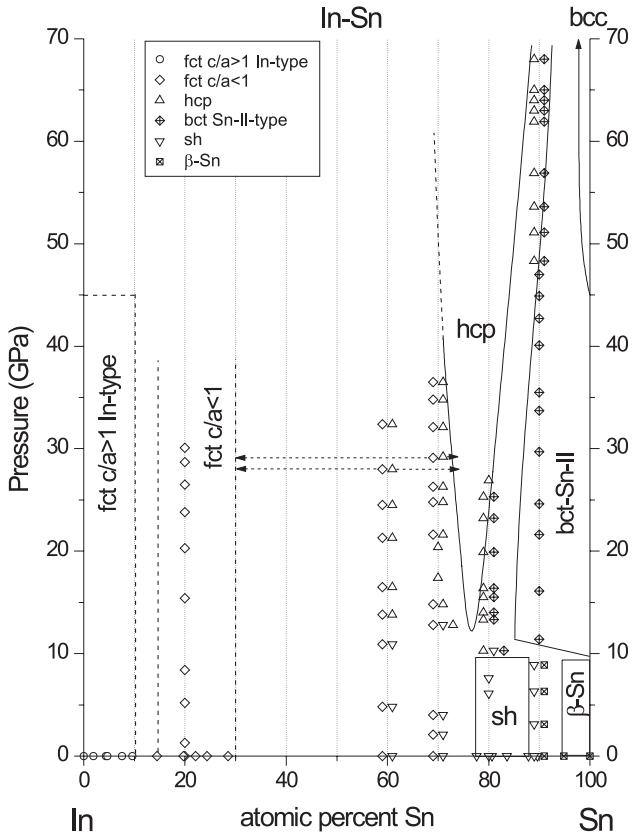

Figure 8. A P–x diagram of the phase regions for the In–Sn alloy system. Different symbols in the phase diagram denote experimental points for the alloys studied, corresponding to different phases observed. Present ambient-pressure and high-pressure data are shown together with ambient-pressure data for the alloys [9]. Transition pressures for pure Sn and In are taken from [14, 17]. Two (or three) symbols at one point indicate a phase mixture, where the corresponding composition of the phases is shown by horizontal arrows. The regions of phase stability are determined from atomic volume considerations.

In this high-pressure experiment at ambient temperature no intermediate phases were noticed, and therefore another run with this alloy was performed with heating under pressure.

The cell with the sample was heated at pressure 16.3 GPa up to a temperature of 150 °C for 1 h. This procedure did not result in any noticeable change and the same two-phase mixture with bct Ga and bct Sn was observed after cooling under pressure. To accelerate the kinetic process the pressure in the cell was decreased down to 11.4 GPa, and the sample was heated to 150 °C again for about 1.5 h. A diffraction pattern taken at room temperature at 11.4 GPa after this heating revealed a new phase with a sh structure together with a small number of bct Ga diffraction peaks. The sh phase is then maintained on further increase of pressure up to 23.8 GPa, the maximum pressure in this run, coexisting with bct Ga. For the sh phase the lattice parameters are $a = 299.5(2)$ pm, $c = 277.9(3)$ pm, and $c/a = 0.928$ at 11.4 GPa. The composition of the sh phase is probably close to 15–18 at.% Ga.

On decompression, the sh phase is retained down to 4–5 GPa, where the diffraction peaks of β-Sn appear. This indicates a hysteresis in pressure for the sh phase formation and decomposition.

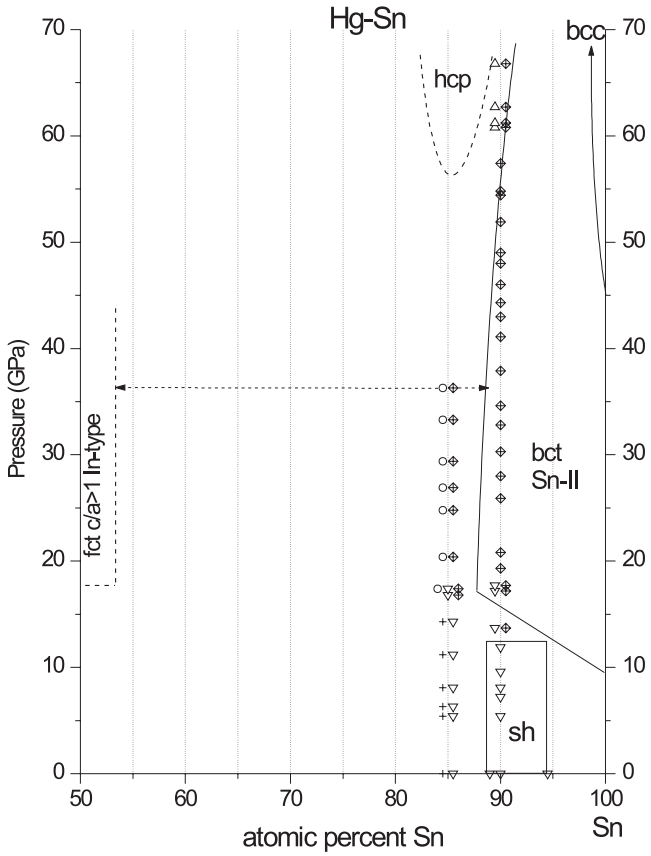

Figure 9. A P–x partial diagram of the phase regions for the Hg–Sn alloy system in the composition range from 50 to 100 at.% Sn. The symbols have the same meaning as in figure 8. An additional symbol, '+', denotes an admixture of another phase with undetermined structure.

4. Discussion

High pressure affects the phase equilibria in a binary alloy system producing an extension of solid solutions, phase decomposition and formation of new intermediate phases of metallic type [1]. The phases observed in the systems studied are discussed below, considering their stability with respect to pressure and alloy composition.

The sh phase. In the In–Sn system the sh phase exists at ambient pressure in the composition range ∼75 to ∼87 at.% Sn and is retained under pressures up to 13 GPa at room temperature. The axial ratio c/a slightly increases with pressure, going from 0.932 to 0.934 ($In_{20}Sn_{80}$) [11]. In the Hg–Sn system the sh phase exists under ambient conditions in the composition range ∼89–94.5 at.% Sn, and is retained under pressure up to ∼15 GPa at room temperature. The axial ratio slightly increases with pressure from 0.930 to 0.934 ($Hg_{10}Sn_{90}$) [13]. For these two alloy systems this means that the sh phase appears to be stable under pressures up to 13–15 GPa in the valence electron concentration range of about 3.8–3.9 electrons/atom and this range does not vary significantly with pressure, at least without heating.

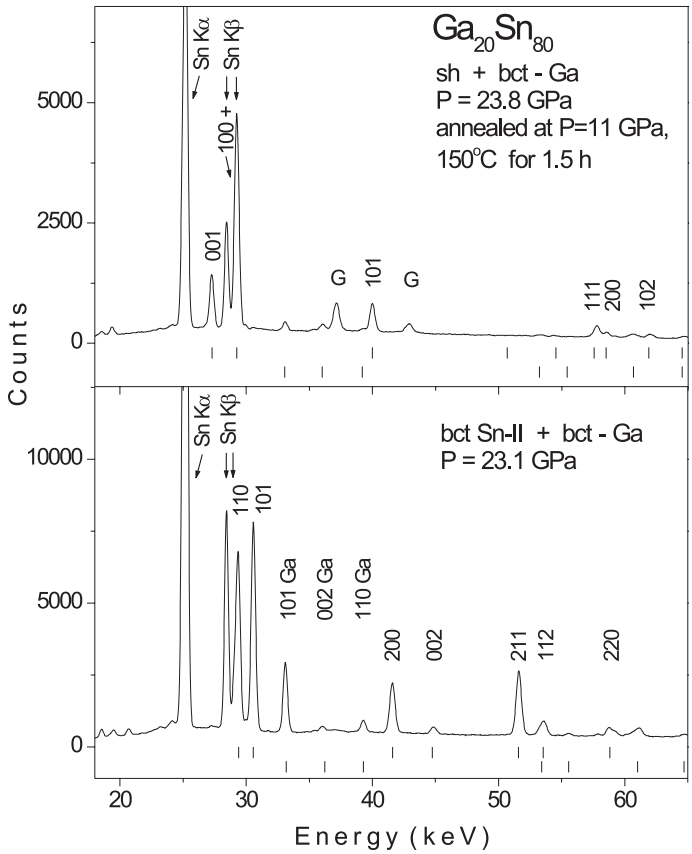

Figure 10. EDXD spectra for the $Ga_{20}Sn_{80}$ alloy collected with $2\theta = 9.63^\circ$ ($Ed = 7383$ keV pm). The pattern at 23.1 GPa corresponds to a two-phase mixture: bct Sn II with $a = 355.1(2)$ pm, $c = 330.0(3)$ pm, $c/a = 0.929$ (peaks hkl); and bct Ga with $a = 265.7(4)$ pm, $c = 407.6(6)$ pm (peaks hkl Ga). After pressure decrease to 11.4 GPa and heating to 150 °C for 1 h 40 min the pattern corresponds to: sh and bct Ga at 23.8 GPa with $a = 291.5(2)$ pm, $c = 270.7(2)$ pm, $c/a = 0.929$ for the sh phase (peaks hkl); and $a = 266.4(12)$ pm, $c = 410.2(6)$ pm for the bct Ga phase. The calculated peak positions are shown as tick marks below each pattern. 'G' denotes diffraction peaks from the gasket material.

A new intermediate phase with sh structure occurs in the Ga–Sn system under pressure with an axial ratio $c/a = 0.928$ at 11.4 GPa. This phase is retained under pressure up to at least 23.8 GPa, with the axial ratio increasing only slightly up to $c/a = 0.930$. The sh phase occurs in the Ga–Sn system at compositions around 82–85% Sn, i.e. at a valence electron concentration of about 3.85 electrons/atom.

To the family of sh phases also belong intermediate high-pressure phases in the Al–Ge, Cd–Sb and Zn–Sb systems [1, 23, 24]. In the light group IV elements Si and Ge the sh phase occurs under high pressure as a post-*white-tin* phase [25–27].

Thus, the sh phase in these alloys and elements appears to have some specific features: a special value of the valence electron concentration of 3.7–4 electrons/atom and a special value of the axial ratio around $c/a = 0.930$.

A recent observation of a sh phase in the group V element P under very high pressures above 137 GPa [28] indicates a possible expansion of the stability range for the sh phase to

higher valency for lighter elements. On the other hand, this can indicate a valence electron hybridization in P on very strong compression.

The hcp phase. The stability range of the high-pressure hcp phase in the In–Sn system is located around 3.75 electrons/atom—apparently similar to the stability range for the hcp phase in Hg–Sn alloys, where it is shifted to somewhat higher pressures. This corresponds to the observation of hcp structure in the $Al_{30}Ge_{70}$ alloy as a post-sh phase [23]. However, this phase was observed in pure Si at pressures above 40 GPa [25] and in Ge above 160 GPa [29], which implies an extension of the hcp region to 4 electrons/atom in the lighter materials. A hcp phase is also a high-pressure form for the heaviest group IV element Pb with a nearly ideal axial ratio.

The experimental studies on Sn show stability of the bcc structure up to at least 120 GPa and no transformation to hcp structure [30]. However, theoretical calculations [31] indicate very close crystal structure energies for the three structures hcp, bct and bcc. Therefore the appearance of the hcp phase in Sn with an addition of Hg or In provides a link to the hcp stability field in lighter and heavier group IV elements.

The fct (In-type) phase; $c/a > 1$. An intermediate phase with the fct structure of In type with $c/a > 1$ appears in the Hg–Sn alloy system under pressure as an intermediate phase around the alloy composition 50/50. This alloy composition implies a valence electron concentration of about 3 electrons/atom for this phase. The $Hg_{50}Sn_{50}$ fct phase together with the fct phases in the elements In and Ga determine the stability range of this phase to be around 3 electrons/atom. This example provides additional confirmation of correlations between the structure and alloy electron concentration in these systems. Further investigations on more enriched Hg alloys are necessary to determine the exact stability range of the fct phase.

The In-type structure in Hg–Sn alloy appears under pressure with an axial ratio $c/a = 1.075$ (in the fct setting), which decreases with pressure slightly to 1.065. These c/a values are very close to those observed in fct structures in Ga under high pressure and in In itself. In indium, c/a increases first from 1.075 up to 1.092, and then decreases slightly [17,18] whereas, in Ga, it decreases with pressure from 1.11 down to the value of 1 for the fcc structure [21,22]. All these fct phases have the specific feature of appearing with an axial ratio close to $c/a = 1.1$, which has a tendency to decrease with increasing pressure.

The fct′ phase; $c/a < 1$. This phase is stable at ambient and high pressure in In–Sn alloys at the alloy composition 15–30 at.% Sn with an axial ratio close to $c/a = 0.93$. From the similarity to the In–Sn system a possible formation of the fct′ phase with $c/a < 1$ is expected in Hg–Sn systems at higher pressures.

An expansion of the fct′ stability region under pressure has been recently reported for In–Pb alloys [12]. Thus the fct′ phase appears to be stable under pressure in the electron concentration range ∼3.2–3.6 electrons/atom. The fct′ structure shows a correlation between the axial ratio and the number of valence electrons. The axial ratio decreases (the degree of tetragonal distortion from the fcc structure increases) with increasing electron concentration and with increasing pressure [12].

The bct (Sn II-type) phase. This phase was first observed in pure Sn [32] with $c/a = 0.92$–0.95 as a high-pressure phase existing before a transition to the bcc structure [14]. A similar phase has been found under pressure in the isoelectronic III–V compound InBi [33]. In Sn alloys with In and Hg the bct phase occurs at pressures above 13–15 GPa and extends up

to alloy compositions of 15 at.% In and 10 at.% Hg, corresponding to a valence electron concentration 3.8–3.85 electrons/atom. The observation of this bct phase in Sn, Sn alloys and InBi determines the stability range of this phase to be 3.8–4 electrons/atom.

While this bct phase represents a slight distortion of a bcc structure with $c/a < 1$, it demonstrates a direct dependence of c/a on the number of valence electrons n. The axial ratio has the following upper values on pressure increase before the transition to bcc or hcp structure: for Sn and InBi with $n = 4$ the axial ratio is $c/a = 0.95$–0.96 [14,33]; for $In_{10}Sn_{90}$ with $n = 3.9$ the axial ratio is $c/a = 0.927$ (present work); and for $Hg_{10}Sn_{90}$ with $n = 3.8$ the axial ratio is $c/a = 0.92$ [13]. The value of the axial ratio decreases with decreasing valence electron concentration. The electronic reason for the tetragonal distortion of the bcc structure has already been discussed in terms of Brillouin-zone–Fermi-sphere interaction [13, 33].

We should mention that a very recent study on the $In_{25}Sn_{75}$ alloy under pressure [34] found a sequence of transformations on compression from sh to bct + hcp to hcp structure, in agreement with our observations.

5. Conclusions

In the present work, phase transitions under high pressure have been studied for the alloy systems In–Sn, Hg–Sn and Ga–Sn. Phase stability regions have been determined with respect to pressure and electron concentration. All phases have been systemized using the axial ratio of the crystal structure with change of pressure and composition. For the bct and fct phases the tetragonal distortion (axial ratio) was found to correlate with the number of valence electrons in the alloys. Phase sequences with changing valence electron concentration have been established for the range 3–4 electrons/atom at moderate and high pressures.

For the variation of the valence electron concentration from 3 to 4 electrons/atom, the phase sequence fct, $c/a > 1 \rightarrow$ fct$'$, $c/a < 1 \rightarrow$ sh $\rightarrow \beta$-Sn appears at ambient and moderate pressures. At higher pressures the phase sequence changes to fct, $c/a > 1 \rightarrow$ fct$'$, $c/a < 1$ (extended range) $\rightarrow$ hcp $\rightarrow$ bct (bcc). The phase regions correlate with the alloy electron concentration.

Acknowledgments

The authors wish to thank W Sievers and W Bröckling for technical assistance. Financial support by the Russian Foundation for Basic Research under the grant number 01-02-97030 and by the Deutsche Forschungsgemeinschaft under the grant numbers 436 RUS 17/74/99 and Ho486/27-1 is gratefully acknowledged.

References

[1] Ponyatovskii E G and Degtyareva V F 1989 *High Pressure Res.* **1** 163
[2] Massalsky T B 1986 *Binary Alloy Phase Diagrams* (Metals Park, OH: American Society for Metals)
[3] Hansen M and Anderko K 1958 *Constitution of Binary Alloys* (New York: McGraw-Hill) (reprinted (New York: Genium))
[4] Syassen K and Holzapfel W B 1978 *Europhys. Conf. Abstr.* A **1** 75
[5] Holzapfel W B 1989 *Simple Molecular Systems at Very High Density* ed A Polian, P Loubere and N Bocca (New York: Plenum) pp 257–76
[6] Otto J W 1997 *Nucl. Instrum. Methods Phys. Res.* A **384** 552
[7] Mao H K, Bell P M, Shaner J W and Steinberg D J 1978 *J. Appl. Phys.* **49** 3276
[8] Porsch F 1995 *EDXPowd And XPOWDER—the Programs for Evaluation of EDXD Spectra* (Paderborn: RTI)

[9] *A Handbook of Lattice Spacings and Structures of Metals and Alloys* 1964 vol 1, ed W B Pearson (Oxford: Pergamon)
A Handbook of Lattice Spacings and Structures of Metals and Alloys 1967 vol 2, ed W B Pearson (Oxford: Pergamon)
[10] Villars P and Calvert L D 1985 *Pearson's Handbook of Crystallographic Data for Intermetallic Phases* (Metals Park, OH: American Society for Metals)
[11] Degtyareva V F, Degtyareva O, Holzapfel W B and Takemura K 2000 *Phys. Rev.* B **61** 5823
[12] Degtyareva O, Degtyareva V F, Porsch F and Holzapfel W B 2001 *J. Phys.: Condens. Matter* **13** 7295
[13] Degtyareva V F, Degtyareva O, Winzenick M and Holzapfel W B 1999 *Phys. Rev.* B **59** 6058
[14] Olijnyk H and Holzapfel W B 1984 *J. Physique Coll.* **45** C8 53
[15] Birch F 1978 *J. Geophys. Res.* **83** 1257
[16] Holzapfel W B 1998 *High Pressure Res.* **16** 81
[17] Takemura K 1991 *Phys. Rev.* B **44** 545
[18] Schulte O and Holzapfel W B 1993 *Phys. Rev.* B **48** 767
[19] Schulte O, Nikolaenko A and Holzapfel W B 1991 *High Pressure Res.* **6** 169
[20] Schulte O and Holzapfel W B 1993 *Phys. Rev.* B **48** 14 009
[21] Schulte O and Holzapfel W B 1997 *Phys. Rev.* B **55** 8122
[22] Takemura K, Kobayashi K and Arai M 1998 *Phys. Rev.* B **58** 2482
[23] Degtyareva V F, Porsch F, Ponyatovskii E G and Holzapfel W B 1996 *Phys. Rev.* B **53** 8337
[24] Degtyareva V F, Bdikin I and Khasanov S S 1997 *Fiz. Tverd. Tela* **39** 1509
Degtyareva V F, Bdikin I and Khasanov S S 1997 *Phys. Solid State* **39** 1341
[25] Olijnyk H, Sikka S K and Holzapfel W B 1984 *Phys. Lett.* A **103** 137
[26] Hu J Z and Spain I L 1984 *Solid State Commun.* **51** 263
[27] Vohra Y K, Brister E, Desgreniers S, Ruoff A L, Chang K L and Cohen M L 1986 *Phys. Rev. Lett.* **56** 1944
[28] Akahama Y, Kobayashi M and Kawamura H 1999 *Phys. Rev.* B **59** 8520
[29] Takemura K, Schwarz U, Syassen K, Hanfland M, Christensen N E, Novikov D L and Loa I 2000 *Phys. Rev.* B **62** R10 603
[30] Desgreniers S, Vohra Y K and Ruoff A L 1989 *Phys. Rev.* B **39** 10 359
[31] Corkill J L, Garcia A and Cohen M L 1991 *Phys. Rev.* B **43** 9251
[32] Barnett J D, Bean V E and Hall H T 1966 *J. Appl. Phys.* **37** 875
[33] Degtyareva V F, Winzenick M and Holzapfel W B 1998 *Phys. Rev.* B **57** 4975
[34] Meenakshi S, Vijayakumar V, Godwal B K and Sikka S K 2001 *Phys. Rev.* B **64** 212104